TRANSPORT THEORY AND STATISTICAL PHYSICS, 30(2&3), 169–204 (2001)

ANGULAR QUADRATURES FOR IMPROVED TRANSPORT COMPUTATIONS

I. K. Abu-Shumays

Bettis Atomic Power Laboratory,
RT-Mathematics, ZAP 34DD/RT, P. O. Box 79,
West Mifflin, PA 15122-0079

ABSTRACT

This paper introduces new octant-range angular quadrature formulas for neutron and photon transport computations. The octant-range quadratures are the three-dimensional (3-D) natural analogue of the one-dimensional (1-D) double-Gauss quadrature most suitable for slab problems with a high degree of heterogeneity. The new quadratures are applicable to a wide range of problems, and are especially suitable for problems with material discontinuities at interfaces and corners where it is advantageous to split the unit sphere of possible directions of particle motion into eight distinct octants.

The octant-range quadratures are generalizations to quadruple-range quadrature formulas for two-dimensional (2-D) rectangular x–y geometries introduced by the present author in the 1970s. A mathematical restriction on the previous quadruple-range quadratures is also relaxed in the present paper. As a consequence, improved accuracy is achieved with fewer angular directions, resulting in significant savings in computing cost.

1. INTRODUCTION

The discrete ordinates method, which is the basis for major production transport theory computer programs, approximates integrals of the scattering term of the particle transport equation over all (infinitely many) possible directions of particle motion, by an angular quadrature summation over a finite set of discrete angular directions [1–9]. As a consequence, the number of angular directions chosen, as well as their distribution over the unit sphere, governs overall accuracy. In addition, for localized source problems and for problems with voids and gaps, artificial flux fluctuations called "ray effects" often arise, especially in situations with low in-group scattering to total cross section ratios. Partial remedies for ray effects are available [7]. One way to ameliorate ray effect fluctuations and improve accuracy is to increase the number of angular directions and to tailor the choice of angular quadratures to the class of problems being addressed [1, 2, 6]. The quadruple-range angular quadratures previously developed [2] were demonstrated to be more effective in ameliorating ray effect fluctuations for rectangular x–y problems than standard [8] S_N type quadratures having the same number of ordinates.

The text of the paper [1] presented at the 16th international conference on transport theory described work done at Bettis within the past 26 years to develop angular quadratures suitable for two- and three-dimensional (2-D and 3-D) rectangular x–y and x–y–z geometries, 2-D and 3-D 60° geometries, as well as cylindrical r–z geometry. For brevity, this paper is restricted to Gauss-type quadratures for 2-D and 3-D rectangular geometry. Additional details and examples of other quadratures for different geometries are provided in a local report [1].

For convenience, the angular direction of particle motion Ω will be represented in terms of (a) direction cosines $\Omega = (\Omega_x, \Omega_y, \Omega_z)$ with respect to an x–y–z rectangular coordinate system, or (b) the polar angle θ as measured with respect to the z-axis and the azimuthal angle ϕ as measured with respect to the x-axis, $\Omega = (\theta, \phi)$, $\Omega = (\mu, \phi)$, $\mu = \cos\theta$. The direction cosines are given in terms of the polar and azimuthal angles by the expressions

$$\Omega_x = \sin\theta\cos\phi, \qquad \Omega_y = \sin\theta\sin\phi, \qquad \Omega_z = \cos\theta. \tag{1}$$

Ninety-degree rotations and reflections may result in new quadrature formulas; such new Quadratures will not be discussed further and will be viewed as implicit.

Section 2 of this paper presents general expressions for representing the angular dependence of the neutron or photon flux. Sections 3, 4 and part of Section 5 below develop quadratures based on approximating the angular

MARCEL DEKKER, INC.
270 Madison Avenue, New York, New York 10016

flux and the flux moments of the transport equation by polynomials in the direction cosines Ω_x, Ω_y, Ω_z. For brevity, all of the quadratures discussed below will be developed for the principal octant of the unit sphere

$$\Omega_x \geq 0, \qquad \Omega_y \geq 0, \qquad \Omega_z \geq 0. \tag{2}$$

The angular quadratures developed below can be extended to the entire unit sphere by rotations and reflections.

Note that for convenience for problems with 2-D symmetries, quadratures developed for the principal octant of the unit sphere in Eq. (2) will be referred to interchangeably as octant-range (OR), or quadruple-range (QR) quadratures.

2. ANGULAR DEPENDENCE

The angular flux for the neutron and the photon particle transport equation is a function of three spatial variables, two angular directions, and energy

$$\psi(\underline{x}, \Omega, E) \equiv \psi(\Omega) \equiv \psi(\mu, \phi) \equiv \psi(\theta, \phi) \equiv \psi(\Omega_x, \Omega_y, \Omega_z). \tag{3}$$

The spatial and energy variables are suppressed in parts of Eq. (3) and will be suppressed below for brevity. Note that the direction cosines in Eq. (3) satisfy the trigonometric relationship

$$\Omega_x^2 + \Omega_y^2 + \Omega_z^2 = 1, \tag{4}$$

and thus the three angular direction cosines in Eq. (3) are coupled.

Earlier treatment [2] established that the vector flux representation for particle transport in x–y geometry has the functional relationship

$$\psi(\Omega) \equiv \psi(\Omega_x, \Omega_y), \tag{5}$$

and does not depend explicitly on Ω_z. Equation (5) follows from: (i) the fact that two-dimensional symmetry with respect to the x–y plane implies that the angular flux (and all flux moments) must be an even function in Ω_z (i.e., must be a function of Ω_z^2), and (ii) dependence of such functions on Ω_z^2 can be eliminated based on Eq. (4).

The functional dependence on direction cosines as expressed in Eqs. (3) and (5) also holds for flux moments. Thus, as is established in previous work [2], transport problems in x–y and x–y–z rectangular geometries involve

MARCEL DEKKER, INC.
270 Madison Avenue, New York, New York 10016

evaluating integrals of the general form

$$\int_{\{\Omega\}} f(\Omega_x, \Omega_y)\, d\Omega, \qquad \int_{\{\Omega\}} f(\Omega_x, \Omega_y, \Omega_z)\, d\Omega, \tag{6}$$

where the range of integration $\{\Omega\}$ stands for the unit sphere of angular directions. The previous work derived angular quadrature formulas based on the reasonable assumption that $f(\Omega_x, \Omega_y)$ in Eq. (6) can be well approximated by polynomials or by piece-wise polynomials in Ω_x and Ω_y. Quadrature formulas in Ref. [2] are given in the form

$$\int_{\{\Omega\}} f(\Omega_x, \Omega_y)\, d\Omega \approx \sum_{m=1}^{N} w_m f(\Omega_x^m, \Omega_y^m). \tag{7}$$

Formulas for the angular ordinates Ω_x^m, Ω_y^m and corresponding quadrature weights w_m in Eq. (7) were derived [2] such that, for each value of N, the approximation in Eq. (7) is rendered exact for the integral in Eq. (6) for polynomials or piecewise polynomials of as high a degree in Ω_x and Ω_y as possible. Quadruple-range (QR) quadratures suitable for rectangular x–y geometry were derived in Ref. [2] by restricting the range of the integrals in Eq. (7) to one quadrant of the unit sphere.

Of particular interest here are quadrature formulas applicable to each octant of the unit sphere of the form

$$\int_{\{\Omega\}/8} f(\Omega)\, d\Omega \approx \sum_{m=1}^{M} w_m f(\Omega^m) = \sum_{m=1}^{M} w_m f(\Omega_{mx}, \Omega_{my}, \Omega_{mz}), \tag{8}$$

where $\{\Omega\}/8$ stands for an octant of the unit sphere. The quadrature formulas based on Eq. (8) will be referred to as octant-range (OR) quadratures. Note that for 2-D rectangular geometry with symmetry with respect to the x–y plane, the quadruple-range quadratures previously developed [2] can also be viewed as octant-range quadratures.

For convenience and to allow for reflecting boundary conditions for rectangular subdivisions in x–y geometry, it is customary to choose principal directions $\Omega_x^m > 0$, $\Omega_y^m > 0$ for $m = 1, \ldots, M$, and to construct a total of $N = 4M$ angular directions of the form

$$\begin{aligned} &\Omega^m = (\Omega_x^m, \Omega_y^m), \qquad \Omega^{m+M} = (-\Omega_x^m, \Omega_y^m), \\ &\Omega^{m+2M} = (-\Omega_x^m, -\Omega_y^m), \qquad \Omega^{m+M} = (\Omega_x^m, -\Omega_y^m), \\ &\Omega_x^m > 0, \qquad \Omega_x^m > 0, \ m = 1, \ldots, M. \end{aligned} \tag{9a}$$

The associated quadrature weights are also required to satisfy

$$w_m = w_{m+M} = w_{m+2M} = w_{m+3M}. \tag{9b}$$

MARCEL DEKKER, INC.
270 Madison Avenue, New York, New York 10016

It is also helpful for x–y and x–y–z problems to reorder the angles in the principal octant such that Ω^m and Ω^{M+1-m} are symmetric pairs of the form

$$\Omega^m = (\Omega_x^m\,,\ \Omega_y^m), \qquad \Omega^{M+1-m} = (\Omega_y^m\,,\ \Omega_x^m), \quad m = 1, \ldots, M. \tag{9c}$$

Equation (9c) is particularly useful for problems with 90-degree rotational boundary conditions.

The octant-range quadratures for x–y–z problems can be extended to the unit sphere in a similar manner. Details will be omitted for brevity.

3. POLYNOMIALS IN DIRECTION COSINES

The main assumption in this section is that the angular integrands of functions of the form $f(\Omega)$ such as given in Eqs. (5)–(8), which arise in the discrete ordinates transport computations, can be well approximated by polynomials in the direction cosines. This assumption leads to "series of integrals" of the following form over the principal octant of the unit sphere:

(a) For rectangular x–y geometry: The integrals corresponding to Eqs. (6) and (7) include the following typical terms in the expansion

$$\begin{aligned}
&\int_{\{\Omega\}/8} (\Omega_x)^l (\Omega_y)^m d\Omega \\
&\quad = \int_0^{\pi/2} d\phi \int_0^{\pi/2} d\theta \sin\theta (\sin\theta\cos\phi)^l (\sin\theta\sin\phi)^m \\
&\quad = \left\{ \int_0^{\pi/2} d\phi\, \cos^l\phi \sin^m\phi \right\} \times \left\{ \int_0^{\pi/2} d\theta\, \sin\theta \sin^{l+m}\theta \right\}, \\
&\qquad l + m \le L.
\end{aligned} \tag{10}$$

where L represents the order of the polynomial approximation of the angular flux.

(b) For rectangular x–y–z geometry: The integrals corresponding to Eqs. (3) and (8) include the following typical terms in the expansion

$$\begin{aligned}
\int_{\{\Omega\}/8} (\Omega_x)^l (\Omega_y)^m (\Omega_z)^n d\Omega = \int_0^{\pi/2} d\phi \int_0^{\pi/2} d\theta \sin\theta (\sin\theta\cos\phi)^l \\
\times (\sin\theta\sin\phi)^m (\cos\theta)^n
\end{aligned}$$

$$= \left\{ \int_0^{\pi/2} d\phi \cos^l \phi \sin^m \phi \right\} \times \left\{ \int_0^{\pi/2} d\theta \sin\theta \sin^{l+m} \theta \cos^n \theta \right\}, \quad l + m + n \leq L. \tag{11}$$

Note that each of the integrals under consideration in Eqs. (10) and (11) is split into a product of two integrals, one over the azimuthal direction and one over the polar direction. The product integrals in Eqs. (10) and (11) involve three distinct functional forms:

(i) Integrals over the azimuthal directions in rectangular 2-D and 3-D geometries given by the identity

$$\int_0^{\pi/2} d\phi \cos^l \phi \sin^m \phi = \Gamma\left(\frac{l+1}{2}\right)\Gamma\left(\frac{m+1}{2}\right) \Big/ 2\Gamma\left(\frac{l+m+2}{2}\right), \tag{12}$$

where $\Gamma(\nu)$is the well known Gamma-function,

(ii) Integrals over the polar angles in 3-D x–y–z rectangular geometry given by

$$\int_0^{\pi/2} d\theta \sin\theta \sin^l \theta \cos^m \theta = \Gamma\left(\frac{l+2}{2}\right)\Gamma\left(\frac{m+1}{2}\right) \Big/ 2\Gamma\left(\frac{l+m+3}{2}\right), \tag{13}$$

(iii) Integrals over the polar angles in 2-D x–y geometry given by

$$\int_0^{\pi/2} d\theta \sin\theta \sin^j \theta = \int_0^1 x^j \frac{x\,dx}{(1-x^2)^{1/2}} = \sqrt{\pi}\,\Gamma\left(\frac{j+2}{2}\right) \Big/ 2\,\Gamma\left(\frac{j+3}{2}\right). \tag{14}$$

Equations (12)–(14) form the basis for octant-range quadratures.

4. GAUSS TYPE QUADRATURES FOR RECTANGULAR *X–Y* AND *X–Y–Z* GEOMETRIES

Separate quadratures will be presented here for integrals over the azimuthal and polar directions involved in transport approximations. Three such quadratures matching Eq. (8) are for integrals along the

azimuthal direction corresponding in part to Eqs. (12) and (18), and two are for integrals along the polar directions corresponding to Eqs. (13) and (14).

(a) The octant-range quadrature sought for the azimuthal direction is of the form

$$\int_0^{\pi/2} f(\cos\phi,\ \sin\phi)d\phi \approx \sum_{i=1}^{M} w_i f(\cos\phi_i,\ \sin\phi_i). \tag{15}$$

Three sets of angular directions ϕ_i and weights w_i were determined in Ref. [2] based on the requirement that the approximation in Eq. (15) be exact for integrating polynomials in Eq. (12) of as high a degree in l and m as possible. To maintain numerical accuracy, previous published work [2] was restricted to $N \leq 7$. This quadrature was referred to as quadruple-range [2] quadrature since it corresponds to subdividing the range of $\phi \in [0, 2\pi]$ into four equal parts. Of particular interest here is the quadruple-range quadrature for the azimuthal direction $\phi \in [0, \pi/2]$ which is symmetric with respect to $\phi = \pi/4$, the 45-degree angle, and thus suitable for implementing 90 degree rotational boundary conditions. This quadrature satisfies the following requirements

$$\phi_{M+1-i} \equiv \frac{\pi}{2} - \phi_i, \quad \phi_i \leq \pi/4, \quad w_{M+1-i} \equiv w_i, \qquad i \leq (M+1)/2. \tag{16}$$

The advantage of symmetry in Eq. (16) is that it results in a factor of 2 reduction in the number of unknown coordinates and weights ϕ_i, w_i that need to be computed for Eq. (15) for each fixed N. Symmetry also results in improved numerical stability. Table 1 extends the results in Ref. [2, p. 308, Table III] for this quadrature from $N \leq 7$ to $N = 22$. Details of the derivation follow below.

It can be shown based on trigonometric identities that for the symmetric case corresponding to Eq. (16), the integrands in Eq. (12) are not all independent and that it suffices to consider only the following integrands

$$\sin^{4k}\phi, \quad \sin^{2k+1}\phi, \quad \sin^{4k+1}\phi\cos\phi, \qquad k = 0, 1, \ldots \tag{17}$$

Substituting the terms from Eq. (17) into Eq. (12) and using identities of the Gamma-functions indicate that the moment equations of interest are of the following forms

$$\int_0^{\pi/2} \sin^{4k+1}\phi\cos\phi\, d\phi = \frac{1}{4k+2}, \tag{18a}$$

$$\int_0^{\pi/2} \sin^{2k+1}\phi d\phi = \frac{2^{\mathrm{k}}\, k!}{1.3.5\cdots(2k+1)}, \tag{18b}$$

Table 1. Quadratures for Azimuthal Integration in Rectangular 2-D and 3-D Geometries: QR Quadratures for Integral of $F(\cos\phi, \sin\phi)$, $0 < \phi < \pi/2$. $\omega(x) = 1$, X(I), W(I) Symmetric w.r.t. $\phi = \pi/4$, X(I) = sinϕ(I) or X(I) = cosϕ(I)

X(I)	W(I)	X(I)	W(I)
$N = 1$		$N = 8$	
7.07106781187E-01	1.57079632679E+00	3.24869788463E-02	8.26105878919E-02
$N = 2$		1.63951256940E-01	1.78010819682E-01
3.28861319306E-01	7.85398163397E-01	3.70037938547E-01	2.45365013149E-01
9.44378225429E-01	7.85398163397E-01	6.00618666309E-01	2.79411742675E-01
$N = 3$		7.99535626274E-01	2.79411742675E-01
1.79705750550E-01	4.41492408805E-01	9.29016643573E-01	2.45365013149E-01
7.07106781187E-01	6.87811509185E-01	9.86468441131E-01	1.78010819682E-01
9.83720409069E-01	4.41492408805E-01	9.99472158795E-01	8.26105878919E-02
$N = 4$		$N = 9$	
1.11919417802E-01	2.79049509269E-01	2.60886177621E-02	6.64555994585E-02
4.99008815360E-01	5.06348654128E-01	1.32824656907E-01	1.45296593486E-01
8.66596908714E-01	5.06348654128E-01	3.05325234799E-01	2.05144486413E-01
9.93717285710E-01	2.79049509269E-01	5.10423681971E-01	2.41615952092E-01
$N = 5$		7.07106781187E-01	2.53771063895E-01
7.60839341001E-02	1.91320724703E-01	8.59923057537E-01	2.41615952092E-01
3.59915255224E-01	3.74855576614E-01	9.52248129951E-01	2.05144486413E-01
7.07106781187E-01	4.38443724162E-01	9.91139551485E-01	1.45296593486E-01
9.32984999374E-01	3.74855576614E-01	9.99659634087E-01	6.64555994585E-02
9.97101416593E-01	1.91320724703E-01	$N = 10$	
$N = 6$		2.14063664984E-02	5.45988342772E-02
5.49823833982E-02	1.38991227102E-01	1.09678208079E-01	1.20668935327E-01
2.68645060598E-01	2.84984797595E-01	2.55406277071E-01	1.73450649536E-01
5.65871339345E-01	3.61422138701E-01	4.35996579025E-01	2.09351736725E-01
8.24493558076E-01	3.61422138701E-01	6.21758783706E-01	2.27328007532E-01
9.63239238931E-01	2.84984797595E-01	7.83208793927E-01	2.27328007532E-01
9.98487324665E-01	1.38991227102E-01	8.99948322449E-01	2.09351736725E-01
$N = 7$		9.66833819037E-01	1.73450649536E-01
4.15504673952E-02	1.05403262712E-01	9.93967147683E-01	1.20668935327E-01
2.07031268158E-01	2.22573419243E-01	9.99770857484E-01	5.45988342772E-02
4.54812160314E-01	2.96659466192E-01		
7.07106781187E-01	3.21524030502E-01		
8.90587389778E-01	2.96659466192E-01		
9.78334326294E-01	2.22573419243E-01		
9.99136406433E-01	1.05403262712E-01		

(*continued*)

Table 1. Continued

X(I)	W(I)	X(I)	W(I)
$N=11$		$N=14$	
1.78781812798E-02	4.56447136792E-02	1.12866459910E-02	2.88696539886E-02
9.20337735274E-02	1.01713727266E-01	5.86080282593E-02	6.53481659572E-02
2.16363520647E-01	1.48226563396E-01	1.40159297798E-01	9.77815191598E-02
3.75037367368E-01	1.82261253182E-01	2.49653542335E-01	1.24592860221E-01
5.46424732468E-01	2.02761156967E-01	3.78014529413E-01	1.44949862586E-01
7.07106781187E-01	2.09581497814E-01	5.14104408362E-01	1.58538699832E-01
8.37508215928E-01	2.02761156967E-01	6.46095281689E-01	1.65317401653E-01
9.27009694166E-01	1.82261253182E-01	7.63256763467E-01	1.65317401653E-01
9.76312873485E-01	1.48226563396E-01	8.57727612534E-01	1.58538699832E-01
9.95755886013E-01	1.01713727266E-01	9.25799662752E-01	1.44949862586E-01
9.99840172545E-01	4.56447136792E-02	9.68335225425E-01	1.24592860221E-01
$N=12$		9.90128966974E-01	9.77815191598E-02
1.51542763381E-02	3.87199557399E-02	9.98281072155E-01	6.53481659572E-02
7.82933178482E-02	8.68389882482E-02	9.99936303783E-01	2.88696539886E-02
1.85385682416E-01	1.27922016108E-01	$N=15$	
3.25051390048E-01	1.59596288800E-01	9.88545479889E-03	2.52957570834E-02
4.81334101720E-01	1.80853870486E-01	5.14258427096E-02	5.74524794603E-02
6.35937834851E-01	1.91467044015E-01	1.23417452644E-01	8.64651177202E-02
7.71740286758E-01	1.91467044015E-01	2.21052006416E-01	1.11038832659E-01
8.76537211145E-01	1.80853870486E-01	3.37331340616E-01	1.30436640770E-01
9.45696353925E-01	1.59596288800E-01	4.63490786372E-01	1.44335592135E-01
9.82665837788E-01	1.27922016108E-01	5.89865690428E-01	1.52659571621E-01
9.96930366866E-01	8.68389882482E-02	7.07106781187E-01	1.55428343897E-01
9.99885167361E-01	3.87199557399E-02	8.07501372913E-01	1.52659571621E-01
$N=13$		8.86101738486E-01	1.44335592135E-01
1.30078426034E-02	3.32559161972E-02	9.41385981751E-01	1.30436640770E-01
6.73938148498E-02	7.49665892004E-02	9.75262021438E-01	1.11038832659E-01
1.60465382602E-01	1.11389848018E-01	9.92354841971E-01	8.64651177202E-02
2.83850626570E-01	1.40595290324E-01	9.98676815943E-01	5.74524794603E-02
4.25605349674E-01	1.61656324749E-01	9.99951137698E-01	2.52957570834E-02
5.71479597861E-01	1.74288947541E-01		
7.07106781187E-01	1.78490494733E-01		
8.20616274045E-01	1.74288947541E-01		
9.04908882888E-01	1.61656324749E-01		
9.58868511213E-01	1.40595290324E-01		
9.87041468727E-01	1.11389848018E-01		
9.97726452351E-01	7.49665892004E-02		
9.99915394436E-01	3.32559161972E-02		

(*continued*)

Table 1. Continued

X(I)	W(I)	X(I)	W(I)
$N = 16$		$N = 18$	
8.72965710742E-03	2.23456344014E-02	6.95206352986E-03	1.78046165668E-02
4.54813865221E-02	5.08947121298E-02	3.63035575806E-02	4.07286438944E-02
1.09465718192E-01	7.69654619574E-02	8.77589835173E-02	6.20554963558E-02
1.96944891481E-01	9.94883219743E-02	1.58962438822E-01	8.10416378981E-02
3.02448274604E-01	1.17816372561E-01	2.46443244015E-01	9.71946843126E-02
4.19021114815E-01	1.31631849523E-01	3.45703234725E-01	1.10230341949E-01
5.38777013625E-01	1.40833201160E-01	4.51447239310E-01	1.20021162996E-01
6.53724513962E-01	1.45422609690E-01	5.57970321081E-01	1.26535909639E-01
7.56732621105E-01	1.45422609690E-01	6.59662846613E-01	1.29785669785E-01
8.42448413607E-01	1.40833201160E-01	7.51561660011E-01	1.29785669785E-01
9.07976489420E-01	1.31631849523E-01	8.29860904485E-01	1.26535909639E-01
9.53165799423E-01	1.17816372561E-01	8.92297814701E-01	1.20021162996E-01
9.80414560132E-01	9.94883219743E-02	9.38343899378E-01	1.10230341949E-01
9.93990571656E-01	7.69654619574E-02	9.69157225366E-01	9.71946843126E-02
9.98965186320E-01	5.08947121298E-02	9.87284631220E-01	8.10416378981E-02
9.99961895817E-01	2.23456344014E-02	9.96141737311E-01	6.20554963558E-02
$N = 17$		9.99340808587E-01	4.07286438944E-02
7.76516751178E-03	1.98823343503E-02	9.99975834114E-01	1.78046165668E-02
4.05069844047E-02	4.53909784761E-02	$N = 19$	
9.77254732972E-02	6.89213492840E-02	6.25951928174E-03	1.60342230649E-02
1.76472506876E-01	8.95844718130E-02	3.27165178199E-02	3.67417542903E-02
2.72416454329E-01	1.06815271243E-01	7.92219146827E-02	5.61476310279E-02
3.79989298340E-01	1.20310163196E-01	1.43872133508E-01	7.36262534663E-02
4.92742032328E-01	1.29950917520E-01	2.23857123544E-01	8.87486446168E-02
6.03908913692E-01	1.35721804820E-01	3.15511709051E-01	1.01251710769E-01
7.07106781187E-01	1.37641745392E-01	4.14465834283E-01	1.11004006334E-01
7.97053338218E-01	1.35721804820E-01	5.15911914917E-01	1.17961656788E-01
8.70175436092E-01	1.29950917520E-01	6.14970011895E-01	1.22126237364E-01
9.24990882737E-01	1.20310163196E-01	7.07106781187E-01	1.23512091351E-01
9.62179440339E-01	1.06815271243E-01	7.88550495828E-01	1.22126237364E-01
9.84305569585E-01	8.95844718130E-02	8.56641638053E-01	1.17961656788E-01
9.95213410214E-01	6.89213492840E-02	9.10064872530E-01	1.11004006334E-01
9.99179255296E-01	4.53909784761E-02	9.48921683519E-01	1.01251710769E-01
9.99969850632E-01	1.98823343503E-02	9.74621971966E-01	8.87486446168E-02
		9.89596285967E-01	7.36262534663E-02
		9.96857004908E-01	5.61476310279E-02
		9.99464671443E-01	3.67417542903E-02
		9.99980409017E-01	1.60342230649E-02

(*continued*)

MARCEL DEKKER, INC.
270 Madison Avenue, New York, New York 10016

Table 1. Continued

X(I)	W(I)	X(I)	W(I)
$N=20$		$N=21$ (Continued)	
5.67509348883E-03	1.45393921491E-02	9.38418107386E-01	9.59071266252E-02
2.96820847851E-02	3.33596736792E-02	9.65922506185E-01	8.56919279330E-02
7.19670984270E-02	5.10954081947E-02	9.83484163393E-01	7.36350186708E-02
1.30959454476E-01	6.72144228938E-02	9.93382512042E-01	5.99002608724E-02
2.04344253359E-01	8.13447311863E-02	9.98039822423E-01	4.48810132722E-02
2.89096892987E-01	9.32502149372E-02	9.99671069337E-01	2.89516129387E-02
3.81584702597E-01	1.02806017860E-01	9.99988067345E-01	1.25272984288E-02
4.77753713079E-01	1.09965085574E-01	$N=22$	
5.73392143001E-01	1.14724634716E-01	4.15241892965E-03	1.03702865159E-02
6.64444346259E-01	1.17098582207E-01	2.14943983335E-02	2.52171295699E-02
7.47337748762E-01	1.17098582207E-01	5.51949788462E-02	4.17522214778E-02
8.19281056991E-01	1.14724634716E-01	1.04398716322E-01	5.70465053218E-02
8.78493818783E-01	1.09965085574E-01	1.67765936458E-01	7.04500290301E-02
9.24333876229E-01	1.02806017860E-01	2.43263988423E-01	8.38347578417E-02
9.57299841463E-01	9.32502149372E-02	3.28167683038E-01	9.27746889748E-02
9.78899088834E-01	8.13447311863E-02	4.19138577496E-01	1.03667304767E-01
9.91387725001E-01	6.72144228938E-02	5.12304337326E-01	1.05523198981E-01
9.97407006565E-01	5.10954081947E-02	6.03869595918E-01	1.18754396046E-01
9.99559389853E-01	3.33596736792E-02	6.90103150166E-01	7.60076448718E-02
9.99983896527E-01	1.45393921491E-02	7.23711021148E-01	7.60076448718E-02
$N=21$		7.97083126860E-01	1.18754396046E-01
4.88519874076E-03	1.25272984288E-02	8.58803974115E-01	1.05523198981E-01
2.56466982317E-02	2.89516129387E-02	9.07922272474E-01	1.03667304767E-01
6.25820489998E-02	4.48810132722E-02	9.44619485195E-01	9.27746889748E-02
1.14852883153E-01	5.99002608724E-02	9.69960118735E-01	8.38347578417E-02
1.80994199785E-01	7.36350186708E-02	9.85826856281E-01	7.04500290301E-02
2.58831435583E-01	8.56919279330E-02	9.94535523765E-01	5.70465053218E-02
3.45501744902E-01	9.59071266252E-02	9.98475595250E-01	4.17522214778E-02
4.37547785645E-01	1.03872159085E-01	9.99768968732E-01	2.52171295699E-02
5.30993475247E-01	1.09613498442E-01	9.99991378671E-01	1.03702865159E-02
6.22088626086E-01	1.13243736140E-01		
7.07106781187E-01	1.14349021980E-01		
7.82946831716E-01	1.13243736140E-01		
8.47375907874E-01	1.09613498442E-01		
8.99195159728E-01	1.03872159085E-01		

(*continued*)

MARCEL DEKKER, INC.
270 Madison Avenue, New York, New York 10016

$$\int_0^{\pi/2} \sin^{4k} \phi d\phi = \frac{1.3.5 \cdots (4k-1)}{2^{2k+1}(2k)!}. \tag{18c}$$

Equations (18a–c) are used in place of Eq. (12) to develop the desired quadratures. In general, the resulting quadrature for a given N will be of order

$$L = N - 1, \quad (l + m \leq L). \tag{19}$$

For convenience, the coordinates

$$x_i \equiv \sin \phi_i, \quad (1 - x_i^2)^{1/2} = \cos \phi_i, \tag{20}$$

will be used in place of ϕ_i. Now, applying the quadrature formulas of Eq. (15) to the functions in Eqs. (17) and (18) and using symmetry yields a set of "nonlinear" equations in the unknowns. For small values of N, this set of nonlinear equations can be solved efficiently by Newton iterations. This solution method, though simple, is known to be subject to round-off errors and numerical instabilities, and its computation requires a high degree of precision arithmetic [3]. In order to avoid numerical difficulties, previous work [2] was limited to $N \leq 7$. In the present paper, the order of quadratures for azimuthal directions is increased to $N \leq 22$, in an attempt to improve accuracy of transport computations for a large class of problems.

The main reason for the numerical instability is the fact that the terms involved in the system of equations combine various powers of x_i with some ordinates x_i close to zero and others close to 1. Accuracy in this case requires increased precision arithmetic with increased orders of the approximations. A new computer program was written by the author to generate quadratures of degrees up to $N = 22$, utilizing double precision arithmetic on Cray computers. The program monitors the loss of significant figures. Computations with more than double precision are needed for quadratures of order higher than 22. Better methods are being investigated for higher order quadrature [5].

(b) The octant-range quadrature sought for the polar direction in 3-D x–y–z rectangular geometry is of the form

$$\int_0^{\pi/2} f(\sin\theta, \cos\theta) \sin\theta \, d\theta \approx \sum_{j=1}^{N} w_j^k f(\sin\theta_j, \cos\theta_j). \tag{21}$$

Equation (21) is similar to Eq. (15), except for the extra sine function in the Jacobian of the integral on the left-hand side. The task now is to find coordinates and weights which render the approximation in Eq. (21) exact for polynomials as in Eq. (13) of as high a degree as possible. Note that the polynomials in Eq. (13) are not all independent for various values of

MARCEL DEKKER, INC.
270 Madison Avenue, New York, New York 10016

l and m, and are related by the trigonometric identity

$$\sin^2\theta + \cos^2\theta = 1. \tag{22}$$

It can be shown that it is sufficient to consider requiring the quadrature approximation in Eq. (13) to be exact for one of the following sets of independent integrands

$$(\sin^j\theta, \sin^j\theta\cos\theta, \quad j = 0, \ldots, N-1), \tag{23}$$

$$(1, \sin^j\theta), \quad (\sin^{j-2}\theta\cos\theta, \sin^j\theta, \quad j = 2, \ldots, N). \tag{24}$$

Other sets of independent polynomials in the sine and cosine also exist.

It is convenient to transform the trigonometric functions and use

$$x = \cos\theta, \quad \sqrt{1-x^2} = \sin\theta, \tag{25}$$

in place of θ. Applying the quadrature formula in Eq. (21) to integrate the set of functions in Eq. (23) or in Eq. (24), and utilizing the analytic expressions in Eq. (13) yield, for each fixed value of N, a system of $2N$ nonlinear equations in $2N$ unknown ordinates and weights for the right-hand side of Eq. (21). Accurate coordinates and weights corresponding to Eqs. (21), (24) and (25) are given in Table 2. Coordinates and weights corresponding to Eqs. (21), (23) and (25) are omitted for brevity [1].

(c) The octant-range quadrature sought for the polar direction in 2-D x–y rectangular geometry is of the form

$$\int_0^{\pi/2} f(\sin\theta)\sin\theta\, d\theta = \int_0^1 f(x)\frac{x\,dx}{(1-x^2)^{1/2}} \approx \sum_{j=1}^{N} w_j^k f(\sin\theta_j)$$

$$= \sum_{j=1}^{N} w_j^k f(x_j), \quad x \equiv \sin\theta. \tag{26}$$

The quadrature sought is then of the form

$$\int_0^1 f(x)\omega(x)\,dx \approx \sum_{i=1}^{N} w_i f(x_i), \quad \omega(x) = x/(1-x^2)^{1/2}, \; x_i = \sin\theta_i. \tag{27}$$

The corresponding optimal Gauss-Christoffel coordinates and weight for Eq. (27) with $N \leq 7$ were constructed and are tabulated to high accuracy in Ref. [2] based on Ref. [3]. The main idea is to determine x_i and w_i ($w_i \neq \omega(x_i)$) such that the approximation in Eq. (27) is rendered exact for all polynomials

$$f(x) = x^j, \quad j = 0, \ldots, 2N-1. \tag{28}$$

MARCEL DEKKER, INC.
270 Madison Avenue, New York, New York 10016

Table 2. Quadratures for Polar Integration in 3-D x–y–z Geometries. Quadratures for Eqs. (21), (24) and (25) for Integral of $F(\cos\theta, \sin\theta)\sin\theta$, $0 < \theta < \pi/2$, $x = \Omega_z = \mu = \cos\theta$, $0 < x < 1$, $\mathrm{X(I)} = \Omega_z(\mathrm{I}) = \mu(\mathrm{I}) = \cos\theta(\mathrm{I}) =$ Polar cone, $\mathrm{W(I)} =$ Weight

X(I) = Ω_z(I)	W(I)	X(I) = Ω_z(I)	W(I)
$N = 1$		$N = 8$	
6.189908924467E-01	1.000000000000E + 00	9.970063368207E-01	9.809563177794E-03
$N = 2$		9.699517300226E-01	4.993755387300E-02
8.634990514471E-01	3.867606081357E-01	8.879503955450E-01	1.167900832303E-01
2.707467653586E-01	6.132393918643E-01	7.361944193605E-01	1.840077166009E-01
$N = 3$		5.304474814371E-01	2.201579963795E-01
9.420141575125E-01	1.734817853566E-01	3.126552110074E-01	2.067710539408E-01
6.014839209434E-01	4.758504223783E-01	1.323869707831E-01	1.476215292233E-01
1.436154828008E-01	3.506677922651E-01	2.526885705460E-02	6.490450357423E-02
$N = 4$		$N = 9$	
9.692550874731E-01	9.483958290718E-02	9.985935590648E-01	4.687271581718E-03
7.603841957105E-01	3.239509561641E-01	9.848612009152E-01	2.638070556035E-02
3.781223125864E-01	3.911333839368E-01	9.384448738513E-01	6.974359023450E-02
7.288031758736E-02	1.900760769918E-01	8.409695379867E-01	1.259654703863E-01
$N = 5$		6.884671704442E-01	1.763082378214E-01
9.907228027705E-01	3.066865270574E-02	4.968907718281E-01	2.013205178931E-01
9.066754949760E-01	1.520873796776E-01	2.982703761263E-01	1.894159794100E-01
6.763407250056E-01	3.007989398347E-01	1.304306562034E-01	1.407412491186E-01
3.455719708920E-01	3.315500881013E-01	2.572642057725E-02	6.543697799409E-02
7.412304396110E-02	1.848949396807E-01	$N = 10$	
$N = 6$		9.988431905941E-01	3.831690452384E-03
9.934260252776E-01	2.136152921019E-02	9.878187060973E-01	2.096950939459E-02
9.365569210587E-01	1.021655746368E-01	9.512982489952E-01	5.461898814248E-02
7.781929016189E-01	2.139690494731E-01	8.748210152191E-01	9.932946005030E-02
5.233269543727E-01	2.824180551767E-01	7.528387780840E-01	1.433909126899E-01
2.469213715865E-01	2.523904145543E-01	5.927047772245E-01	1.735729930089E-01
5.065384196986E-02	1.276953769490E-01	4.137049559308E-01	1.799419832720E-01
$N = 7$		2.420294039117E-01	1.589187774698E-01
9.957315827450E-01	1.392973976943E-02	1.040133416870E-01	1.136148860623E-01
9.579357169756E-01	6.892898464294E-02	2.032527456069E-02	5.181079945732E-02
8.474708404724E-01	1.540022963383E-01		
6.540152494700E-01	2.268755020184E-01		
4.119940170234E-01	2.459222632522E-01		
1.854112547976E-01	1.963577927660E-01		
3.705166699011E-02	9.398342121276E-02		

(*continued*)

Table 2. Continued

X(I) = Ω_z(I)	W(I)	X(I) = Ω_z(I)	W(I)
$N = 11$		$N = 13$ (Continued)	
9.991302677320E-01	2.884161734127E-03	1.582700765155E-01	1.080243650166E-01
9.907904599945E-01	1.592166778168E-02	6.654296956713E-02	7.381055437147E-02
9.628342127515E-01	4.210429510321E-02	1.288229858096E-02	3.291887234697E-02
9.031675682025E-01	7.836749831056E-02	$N = 14$	
8.053034593427E-01	1.169567716752E-01	9.996558737820E-01	1.147057513783E-03
6.716836707816E-01	1.483035686839E-01	9.962693383644E-01	6.560585266642E-03
5.139106257595E-01	1.641342683895E-01	9.844006381495E-01	1.831225051549E-02
3.501888569958E-01	1.598016376376E-01	9.574371978087E-01	3.662153822498E-02
2.011107021879E-01	1.351922425517E-01	9.095151164539E-01	5.980800643841E-02
8.533860285514E-02	9.405053253703E-02	8.372368352245E-01	8.472257845895E-02
1.656084164276E-02	4.228335559564E-02	7.407906029852E-01	1.074785132224E-01
$N = 12$		6.242752767306E-01	1.242764203624E-01
9.993182903074E-01	2.263464406185E-03	4.952311643392E-01	1.321396462151E-01
9.927399491150E-01	1.260438060930E-02	3.635415417531E-01	1.294179363033E-01
9.704415432003E-01	3.379182957262E-02	2.399856722056E-01	1.159714807527E-01
9.220724109667E-01	6.410234109849E-02	1.347776768636E-01	9.301981285636E-02
8.409912076571E-01	9.808702825277E-02	5.639551887688E-02	6.273486468456E-02
7.271112553886E-01	1.284451713994E-01	1.086656296514E-02	2.778930918493E-02
5.876609071491E-01	1.481987487236E-01	$N = 15$	
4.358871441498E-01	1.525460148381E-01	9.997217860289E-01	9.277955332396E-04
2.882445618572E-01	1.399867016900E-01	9.969770851516E-01	5.324881254380E-03
1.609145368599E-01	1.125198356935E-01	9.873133178911E-01	1.494948831251E-02
6.661300974079E-02	7.486149506603E-02	9.652017991798E-01	3.015294391042E-02
1.271017917531E-02	3.259298864993E-02	9.255042701452E-01	4.982592810351E-02
$N = 13$		8.648133493431E-01	7.168598522528E-02
9.996056789222E-01	1.317932282413E-03	7.823872347417E-01	9.277828135504E-02
9.956783395241E-01	7.651720102310E-03	6.805340155142E-01	1.100543192029E-01
9.817170248781E-01	2.166000129594E-02	5.644276467831E-01	1.209126125418E-01
9.496614980081E-01	4.366484358444E-02	4.414412603907E-01	1.236103228459E-01
8.924880178733E-01	7.129522897898E-02	3.201611900935E-01	1.174821237352E-01
8.066758436297E-01	1.000807915314E-01	2.092924891631E-01	1.029369133400E-01
6.937364298650E-01	1.246517659564E-01	1.166739455867E-01	8.124957900491E-02
5.604409274254E-01	1.400696627407E-01	4.857478250334E-02	5.422386305719E-02
4.178107622661E-01	1.429204365193E-01	9.333807675231E-03	2.388496257768E-02
2.792375210342E-01	1.319338252731E-01		

(*continued*)

Table 2. Continued

$X(I) = \Omega_z(I)$	W(I)	$X(I) = \Omega_z(I)$	W(I)
$N = 16$		$N = 18$	
9.997688033812E-01	7.714118602424E-04	9.998643186575E-01	4.535444460650E-04
9.974817188842E-01	4.443946511975E-03	9.985095657004E-01	2.646122049826E-03
9.893904569635E-01	1.254977819319E-02	9.936394403828E-01	7.618786987172E-03
9.707482915922E-01	2.551711882156E-02	9.821650338648E-01	1.589159962766E-02
9.369723698241E-01	4.260265070016E-02	9.607790068479E-01	2.737618872149E-02
8.847379407654E-01	6.208231592071E-02	9.265617655799E-01	4.139739026261E-02
8.127896715603E-01	8.160983285973E-02	8.775185305293E-01	5.680552361525E-02
7.223510099119E-01	9.864709537668E-02	8.129709750266E-01	7.214957225791E-02
6.171016248194E-01	1.108857393961E-01	7.337588102852E-01	8.587880206166E-02
5.027643330792E-01	1.165977355328E-01	6.422382246552E-01	9.654276634823E-02
3.863961603479E-01	1.148706343615E-01	5.420919860080E-01	1.029641396646E-01
2.755133143512E-01	1.057019241225E-01	4.379889494132E-01	1.043642048301E-01
1.771953459552E-01	8.994684678464E-02	3.351477918895E-01	1.004272305469E-01
9.731207205116E-02	6.912603219075E-02	2.388696773826E-01	9.129808005242E-02
4.001376430336E-02	4.508897765036E-02	1.541052327805E-01	7.751774985588E-02
7.627772606466E-03	1.955795971710E-02	8.511044202699E-02	5.991393459237E-02
$N = 17$		3.522248344992E-02	3.947666553464E-02
9.998496261600E-01	5.033980879584E-04	6.746971030014E-03	1.727769854532E-02
9.983377240080E-01	2.963411954252E-03		
9.928507662419E-01	8.619903084610E-03		
9.798024424910E-01	1.813659400784E-02		
9.553151902739E-01	3.141368012838E-02		
9.160087673050E-01	4.756815316756E-02		
8.597217960590E-01	6.508105325269E-02		
7.860255025427E-01	8.205441506288E-02		
6.964538247577E-01	9.651113160550E-02		
5.944358823670E-01	1.066822953425E-01		
4.849651757731E-01	1.112404525269E-01		
3.740752050608E-01	1.094493588037E-01		
2.682147415396E-01	1.012120443687E-01		
1.736297383459E-01	8.700201391745E-02		
9.591061666473E-02	6.748967807090E-02		
3.889663020451E-02	4.562281589888E-02		
7.709154866395E-03	1.844960071929E-02		

Marcel Dekker, Inc.
270 Madison Avenue, New York, New York 10016

Table 3 provides an extension of the results in Ref. [2, p. 307, Table II] to $N = 10$.

5. COMBINED POLAR AND AZIMUTHAL QUADRATURES

The work in Ref. [2] developed compatible product angular quadratures for 2-D x–y rectangular geometry that possess the same order of mathematical accuracy for the separate polar and azimuthal integrals. An example based on Eqs. (15) for the azimuthal direction, (26) for the polar direction and (10) for the product is given by

$$\int_{\{\Omega\}} f(\Omega_x, \Omega_y)\, d\Omega = \int_0^{2\pi} d\phi \int_0^{\pi} d\theta \sin\theta\, f(\sin\theta\cos\phi, \sin\theta\sin\phi) \approx \sum_{i=1}^{4M} \sum_{j=1}^{N} w_i^l w_j^K\, f(\sin\theta_j\cos\phi_i, \sin\theta_j\sin\phi_i). \tag{29}$$

The distinct weights in Eq. (29) correspond to the distinct azimuthal and polar quadratures.

Compatible angular quadrature formulas derived in Ref. [2] were demonstrated to be superior to previous standard quadratures. The question is: Can we do better? Compatibility requires the selection of identical numbers of azimuthal discrete directions on each of the polar cones; and this selection appears to be wasteful. Unfortunately for transport problems, the coupling of the spatial and angular discretizations and the effect of the numerous known singularities are not clearly understood. Thus, as was concluded in Ref. [2], the most suitable choices of angular quadrature for certain classes of transport problems will have to be based on actual numerical experiments. Numerical experiments were conducted to evaluate the merits of differing quadratures and to seek improved selections for representative practical applications. It was found empirically that the use of product quadratures and the requirement of compatibility in Ref. [2] are too restrictive. The same or higher accuracy can be achieved with fewer, well positioned angular directions. Thus, the requirement of complete separability of azimuthal and polar directions [2] is here relaxed.

The procedure adopted for constructing octant-range quadratures is as follows:

Algorithm 1

(i) Select a quadrature for the polar direction. The polar quadrature selected is viewed as defining distinct angular cones

MARCEL DEKKER, INC.
270 Madison Avenue, New York, New York 10016

Table 3. Quadratures for Polar Integration in 2-D x–y Rectangular Geometries. Quadratures for Integral of $F(\sin\theta)\sin\theta$, $0 < \theta < \pi/2$, or $F(x)\omega(x)$, $\omega(x) = x/(1-x^2)^{1/2}$, $0 < x < 1$, $x = \sin\theta$, X(I), W(I), X(I) = sinθ (I)

X(I)	W(I)	X(I)	W(I)
$N=1$		$N=8$	
7.853981633974E-01	1.000000000000E+00	4.619235546733E-02	3.535298053836E-03
$N=2$		1.495785939930E-01	1.939781153201E-02
3.993735638824E-01	2.505459190576E-01	2.974141685414E-01	5.120081207156E-02
9.144479484660E-01	7.494540809424E-01	4.714033535760E-01	9.615210566300E-02
$N=3$		6.494576043473E-01	1.471910521216E-01
2.311522961279E-01	8.530082397263E-02	8.085613275367E-01	1.956194174053E-01
6.399711962341E-01	3.414562579328E-01	9.279142834478E-01	2.332109926667E-01
9.544967673433E-01	5.732429180946E-01	9.918094732391E-01	2.536925104860E-01
$N=4$		$N=9$	
1.492491465731E-01	3.605010432091E-02	3.738717543137E-02	2.321532538025E-03
4.452174134056E-01	1.651009783738E-01	1.218673184482E-01	1.295685275068E-02
7.657198751837E-01	3.388394165669E-01	2.449791366336E-01	3.503122447209E-02
9.718403838896E-01	4.600095007383E-01	3.944837657444E-01	6.774755109636E-02
$N=5$		5.551788717533E-01	1.073193796372E-01
1.039469054750E-01	1.765116967436E-02	7.104369578734E-01	1.483922364818E-01
3.218997600306E-01	8.726300032090E-02	8.440015993099E-01	1.853051377127E-01
5.925641316724E-01	1.993860321943E-01	9.417816602326E-01	2.130391465706E-01
8.367574981863E-01	3.127359798582E-01	9.934143180700E-01	2.278869387406E-01
9.808766137327E-01	3.829638179523E-01	$N=10$	
$N=6$		3.087344674321E-02	1.585962741949E-03
7.642225770190E-02	9.602183026857E-03	1.011256691908E-01	8.966281037954E-03
2.418380224706E-01	4.982286016750E-02	2.049120334874E-01	2.469133544735E-02
4.624149310771E-01	1.216972042400E-01	3.337559301018E-01	4.884013052964E-02
6.917637890192E-01	2.077474677705E-01	4.769246984678E-01	7.941386493165E-02
8.801887364310E-01	2.835447130159E-01	6.222949084152E-01	1.131174844298E-01
9.861717557162E-01	3.275855717792E-01	7.574090067647E-01	1.461301662904E-01
$N=7$		8.705939190886E-01	1.747226071284E-01
5.849788427341E-02	5.651443322490E-03	9.520192454053E-01	1.957168918510E-01
1.876744099204E-01	3.029834441270E-02	9.945898978712E-01	2.068152756119E-01
3.673808738342E-01	7.742885116751E-02		
5.691413298688E-01	1.397678418675E-01		
7.600739892315E-01	2.041795195416E-01		
9.084990189032E-01	2.566694985682E-01		
9.895378462167E-01	2.860045011201E-01		

Marcel Dekker, Inc.
270 Madison Avenue, New York, New York 10016

and associated weights. The polar weights should sum to one (1.0).

(ii) Select possibly independent azimuthal quadratures for the distinct polar angular cones. While totally different azimuthal quadratures can be selected for the different polar cones, in practice it is convenient to select one type of quadrature, but vary the order (the number of discrete azimuthal angles or azimuthal intervals on the different polar cones).

(iii) Associate with each resulting quadrature ordinate a weight equal to the product of the polar weight corresponding to the polar angle, and the azimuthal weight corresponding to the azimuthal direction and the azimuthal quadrature selected.

The concept embodied in Algorithm 1 is not new [4, 6, 8]. Mixtures of new and old well known polar and azimuthal quadratures were combined and tested.

It cannot be overemphasized that most of the new quadrature combinations applied below were arrived at by trial and error and by several numerical tests. Numerous other choices of angular mesh subdivisions, some based on what a priori seemed to be physically reasonable, resulted in exaggerated ray effects. The quadratures presented and applied in this study are not claimed to be optimal.

(a) Combined polar and azimuthal quadratures for general x–y problems

Experience with x–y transport problems suggests that these problems are more sensitive to the choice of azimuthal directions than polar directions. Since for two dimensional x–y geometries, particles moving close to the z-axis are not expected to contribute as much to transport as particles moving close to the x–y plane, it is advantageous to vary the number of azimuthal directions on separate polar cones and to select more azimuthal directions on cones closer to the x–y plane and less on cones closer to the z-axis. The advantage of varying the distribution of azimuthal angles on the various polar cones as was advocated by Carlson and others [4, 6, 8] is confirmed in the present study.

In the late 1960s, Gelbard and Shure [6] compared numerical results obtained with transport computations using standard S_{16} angular quadratures and a variety of other quadratures, against benchmark computations based on a very high order P_{19} spherical harmonics approximation. They concluded that the choice of 4 double-Gauss cones with 10 angles per octant on the top cone, 11 angles per octant on the second cone, 12 on the third cone, and 14 on the fourth and bottom cone, is appropriate for x–y

problems. They intuitively preferred 4 double-Gauss cones to 4 single-Gauss cones, because the double-Gauss cones are closer to the x–y plane than the corresponding single-Gauss cones. Their four-cone quadrature was demonstrably superior to the standard eight cone S_{16} quadrature and was close enough to their benchmark to justify its adoption in shield design and analysis.

The present paper also confirms previous findings [6] and demonstrates that it is sufficient to consider only 4 polar cone directions. However, improved selection of cones and angular distribution on different cones is provided below.

Four different choices of angular quadratures for the polar direction are considered:

(i) SG – Single-Gauss quadrature in $\mu = \cos\theta$, θ the polar angle,
(ii) DG – Double-Gauss quadrature in μ,
(iii) U – Uniform distribution of μ in the open interval (0, 1), and
(iv) QR – Quadruple-range quadrature in the polar angle θ (Table 3).

The first three are standard quadrature formulas [8, 9]. As far as the polar direction for rectangular x–y problems is concerned, in fact the choice $N = 4$ is appropriate, and $N = 10$ is viewed as providing a benchmark. Increasing N beyond 10 is not expected to change the results.

Three choices of azimuthal angular directions are considered in combination with the above choices for polar directions:

(i) U – Uniform distribution of azimuthal angles on the open interval $\phi \in (0, \pi/2)$,
(ii) QR – Quadruple-Range quadrature in the azimuthal angle ϕ (Table 1), and
(iii) MP – Variable mid-point rule quadrature in the azimuthal direction [1].

The azimuthal distribution however may be different on different polar cones.

The choice of quadrature U corresponding to uniform distribution of discrete directions in the azimuthal angle ϕ over the interval of the unit circle $\phi \in [0, 2\pi]$ is a Chebyshev–Gauss quadrature and is known to be mathematically optimal for functions which are continuous in ϕ over that interval.

The combined polar and azimuthal quadratures tested in the ray effect problem described below, and for other realistic problems, are defined in Table 4. The order in which the non-negative integers i, j, k, and l appear in Table 4 for the quadratures sgijkl, ..., qijkl is not important. It is to be

MARCEL DEKKER, INC.
270 Madison Avenue, New York, New York 10016

understood that, if these integers are reordered in increasing magnitude, then the first and smallest integer would stand for the number of azimuthal angles/octant on the top cone (cone closest to the z-axis), the second integer would stand for the number of azimuthal angles/octant on the second cone from the z-axis, the third integer would stand for the number of azimuthal angles/octant on the third cone from the z-axis, and the fourth and largest integer would stand for the number of azimuthal angles/octant on the bottom cone, which is closest to the x–y plane.

In addition to the angular quadratures listed in Table 4, tests were carried out with analogous uijkl angular quadratures based on polar cones uniformly distributed in $\mu = \cos\theta$, where θ is the polar angle measured from the z-axis. The uniform cone quadratures were experimentally found not to be competitive and are not considered further in this study.

Several useful combinations of known SG, DG, Uniform, and the new octant-range (OR) and composite mid-point rule and Gauss type quadratures for the azimuthal and polar directions appropriate for 3-D problems can be deduced from this study. However, examples, applications and further discussion of quadratures for 3-D and for problems in 60-degree geometry are beyond the scope of the present paper.

(b) Sample angular quadratures for x–y problems

Examples of good angular quadratures for x–y rectangular problems are listed in Tables 5 and 6. Table 5 shows the q461214 quadruple-range quadrature with 4 QR polar cones and with respectively 4, 6, 12, and 14 QR azimuthal angles/octant on top, second, third, and bottom cones (total 36 angles/octant).

Table 6 shows the q2468 quadruple-range quadrature with 4 QR polar cones and with respectively 2, 4, 6, and 8 QR azimuthal angles/octant on top, second, third, and bottom cones (total 20 angles/octant).

Figure 1a shows the q461214 quadruple-range quadrature for visual inspection. Figure 1b shows the subtle differences between the four cone double-Gauss (dg461214, etc.), single-Gauss (sg461214, etc.) and quadruple-range (q461214, etc.) quadratures. The figure shows the location of the cones (projection on the z-axis) and the weights associated with each cone. What matters for x–y problems is not only the locations of the various cones, but also the weights associated with these cones. The QR quadrature has much less weight associated with the cone closest to the z-axis than for the SG quadrature; the SG quadrature in turn has less weight associated with the cone closest to the z-axis than for the DG quadrature. The QR quadrature has much more weight associated with the cone closest to the

MARCEL DEKKER, INC.
270 Madison Avenue, New York, New York 10016

Table 4. Notation for Quadratures for General X–Y Problems

Quadrature	Description
$s16 = S_{16}$	Standard axially invariant symmetric S_{16} quadrature with 36 angles/octant.
sg16 g16	S_{16}-like quadrature with 36 angles/octant based respectively on 8 SG and 8 DG cones, one angle on the top cone closest to the z-axis, two on the second cone,. . ., and eight on the bottom cone closest to the x–y plane. The azimuthal angles on each cone are uniformly distributed.
$sg10 \times 20$ $dg10 \times 20$	Respectively 10 SG and DG polar cone quadratures each with 20 uniformly distributed azimuthal angles/cone/octant. Total 200 angles/octant.
$s10 \times 20$, $d10 \times 20$ $q10 \times 20$	Benchmarks with respectively 10 SG, DG and QR polar cone quadratures each with 20 QR azimuthal anglescone/octant. Total 200 angles/octant.
$sg4 \times 20$ $g4 \times 20$	Respectively 4 SG and DG polar cone quadratures each with 20 uniformly distributed azimuthal angles/cone/octant. Total 80 angles/octant.
$s4 \times 20$, $d4 \times 20$ $q4 \times 20$	Respectively 4 SG, DG and QR polar cone quadratures each with 20 QR azimuthal anglescone/octant. Total 80 angles/octant.
Sgijkl dgijkl	Respectively 4 SG and DG polar cone quadratures each with i, j, k and l uniformly distributed azimuthal angles/octant on the various cones. Total $i+j+k+l$ angles/octant.
Sijkl dijkl qijkl	Respectively 4 SG DG and QR polar cone quadratures each with i, j, k and l QR azimuthal angles/octant on the various cones. Total $i+j+k+l$ angles/octant.
dg10111213 = dg13121110	Four DG polar cones and respectively 10, 11, 12, and 13 uniformly distributed azimuthal angles/octant on top, second, third, and bottom cones. Total 46 angles/octant (Developed by Gelbard and Shure [6]).

x–y-plane than for the SG quadrature; the SG quadrature in turn has more weight associated with the cone closest to the x–y-plane than for the DG quadrature. Since for x–y problems, transport along the z-direction is not as important as transport along x–y, Figure 1b suggests that for such problems, quadruple range distribution of polar cones is to be preferred to single-Gauss which in turn is to be preferred to double-Gauss. Our numerical tests indicate that this is indeed the case.

Table 5. Q36 = q461214 Octant-Range or Quadruple-Range Quadrature for Rectangular x–y Geometry

m	Ω_x^m	Ω_y^m	w_m
1	9.717784813336E-01	1.096881837272E-02	8.454511187252E-03
2	7.656319455497E-01	1.160393058611E-02	8.352354145856E-03
3	4.445439440056E-01	2.447911451942E-02	1.460888798152E-02
4	9.701698603928E-01	5.695764868253E-02	1.913728513580E-02
5	7.633693960835E-01	5.995074957044E-02	1.873220073879E-02
6	1.483114568272E-01	1.670387759191E-02	6.404244616724E-03
7	9.622473153642E-01	1.362124657777E-01	2.863542971348E-02
8	7.524467626583E-01	1.419535016004E-01	2.759429759588E-02
9	9.410672772109E-01	2.426233944222E-01	3.648716160597E-02
10	4.288508824476E-01	1.196054590036E-01	2.995376809966E-02
11	7.241384940891E-01	2.488983098158E-01	3.442681426024E-02
12	8.997294996538E-01	3.673697853806E-01	4.244873302980E-02
13	6.711819639118E-01	3.685670882907E-01	3.901232700510E-02
14	1.293388490485E-01	7.447663982495E-02	1.162080754372E-02
15	8.335743322378E-01	4.996274255819E-01	4.642823955812E-02
16	3.670788892962E-01	2.519357740235E-01	3.798783310581E-02
17	5.909368760506E-01	4.869502395267E-01	4.130171453748E-02
18	7.417637460141E-01	6.279014865859E-01	4.841339013884E-02
19	6.279014865859E-01	7.417637460141E-01	4.841339013884E-02
20	4.869502395267E-01	5.909368760506E-01	4.130171453748E-02
21	2.519357740235E-01	3.670788892962E-01	3.798783310581E-02
22	4.996274255819E-01	8.335743322378E-01	4.642823955812E-02
23	7.447663982495E-02	1.293388490485E-01	1.162080754372E-02
24	3.685670882907E-01	6.711819639118E-01	3.901232700510E-02
25	3.673697853806E-01	8.997294996538E-01	4.244873302980E-02
26	2.488983098158E-01	7.241384940891E-01	3.442681426024E-02
27	1.196054590036E-01	4.288508824476E-01	2.995376809966E-02
28	2.426233944222E-01	9.410672772109E-01	3.648716160597E-02
29	1.419535016004E-01	7.524467626583E-01	2.759429759588E-02
30	1.362124657777E-01	9.622473153642E-01	2.863542971348E-02
31	1.670387759191E-02	1.483114568272E-01	6.404244616724E-03
32	5.995074957044E-02	7.633693960835E-01	1.873220073879E-02
33	5.695764868253E-02	9.701698603928E-01	1.913728513580E-02
34	2.447911451942E-02	4.445439440056E-01	1.460888798152E-02
35	1.160393058611E-02	7.656319455497E-01	8.352354145856E-03
36	1.096881837272E-02	9.717784813336E-01	8.454511187252E-03

Table 6. Q20 = q2468 Octant-Range or Quadruple-Range Quadrature for Rectangular x–y Geometry

m	Ω_x^m	Ω_y^m	w_m
1	9.713274064903E-01	3.157215799340E-02	2.419260514149E-02
2	7.645615896150E-01	4.210110375297E-02	2.998205782366E-02
3	4.424202396002E-01	4.982847370367E-02	2.932993043666E-02
4	9.586898685237E-01	1.593344524838E-01	5.213067212540E-02
5	7.375714298063E-01	2.057068622698E-01	6.147460425028E-02
6	1.409476441875E-01	4.908227124734E-02	1.802505216045E-02
7	9.028558915298E-01	3.596178122512E-01	7.185542471164E-02
8	3.858240341629E-01	2.221674140412E-01	5.322055875020E-02
9	6.313311043797E-01	4.332989313333E-01	7.796304620960E-02
10	7.770210099715E-01	5.837054752370E-01	8.182604839076E-02
11	5.837054752370E-01	7.770210099715E-01	8.182604839076E-02
12	4.332989313333E-01	6.313311043797E-01	7.796304620960E-02
13	2.221674140412E-01	3.858240341629E-01	5.322055875020E-02
14	3.596178122512E-01	9.028558915298E-01	7.185542471164E-02
15	4.908227124734E-02	1.409476441875E-01	1.802505216045E-02
16	2.057068622698E-01	7.375714298063E-01	6.147460425028E-02
17	1.593344524838E-01	9.586898685237E-01	5.213067212540E-02
18	4.982847370367E-02	4.424202396002E-01	2.932993043666E-02
19	4.210110375297E-02	7.645615896150E-01	2.998205782366E-02
20	3.157215799340E-02	9.713274064903E-01	2.419260514149E-02

6. NUMERICAL COMPARISON

As mentioned in Ref. [2], the most suitable choices of angular quadratures for certain classes of transport problems will have to be based on actual numerical experiments. This paper summarizes a detailed comparison of various quadratures for two problems:

(i) A ray effect benchmark problem designed by K. D. Lathop [7] and extensively used to determine quadratures suitable for rectangular x–y transport applications [2], and
(ii) A model problem of a localized square source in a large void compartment designed to determine quadratures suitable for dry cell storage applications.

Additional comparison of quadratures for other problems is provided in a local report [1]. The new quadratures developed for 3-D problems (and for 60-degree geometry [1]) have not been extensively tested to date and further details are beyond the scope of this paper.

MARCEL DEKKER, INC.
270 Madison Avenue, New York, New York 10016

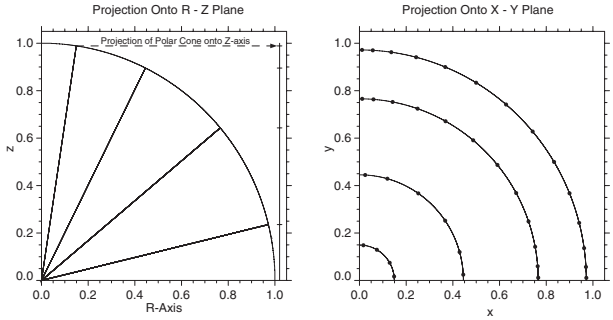

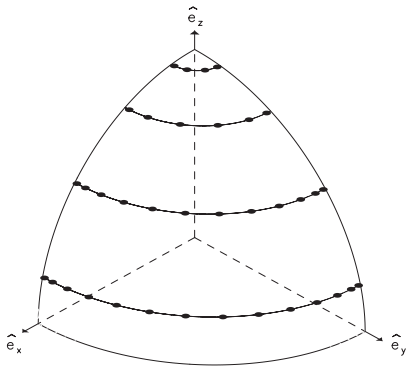

Figure 1a. q4, 6, 12, 14 quadrature.

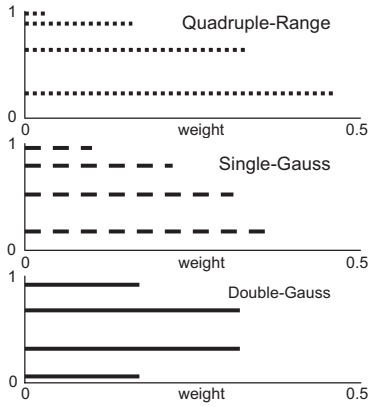

Figure 1b. Weights associated with four cone quadruple-range, single Gauss, and double Gauss quadratures.

(a) Numerical results for benchmark x–y ray effect problem

The ray effect problem is a one-energy-group neutron transport benchmark problem shown in Figure 2. The spatial domain is divided into 30×30 equally spaced mesh intervals $\Delta x=\Delta y=2/30$. The diamond difference discrete-ordinates approximation was applied to solve this problem for various choices of angular quadratures and for two choices of scattering cross sections: $c=\sigma_s/\sigma_t=1/3$, and $c=\sigma_s/\sigma_t=1/10$, c being the number of secondaries per collision. The smaller the $c=\sigma_s/\sigma_t$ ratio, the more pronounced are the ray effect artificial flux fluctuations. It is hard to clearly distinguish between certain quadratures for the case $c=\sigma_s/\sigma_t=1/3$, in contrast with the situation for $c=\sigma_s/\sigma_t=1/10$. Consequently, all the numerical results for $c=\sigma_s/\sigma_t=1/3$ are omitted for brevity.

The net neutron fluxes for the various choices of angular quadratures are compared at the centers of mesh cells and primarily at the centers of the right boundary mesh cells ($x=1.967$) and/or at the centers of the top boundary mesh cells ($y=1.967$). All problems were solved with a convergence criterion

$$\frac{1}{1-\mathrm{ER}}\max_i\frac{\left|\Phi_i^n-\Phi_i^{n-1}\right|}{\Phi_i^n}\le \mathrm{EPS}=10^{-3}, \tag{30}$$

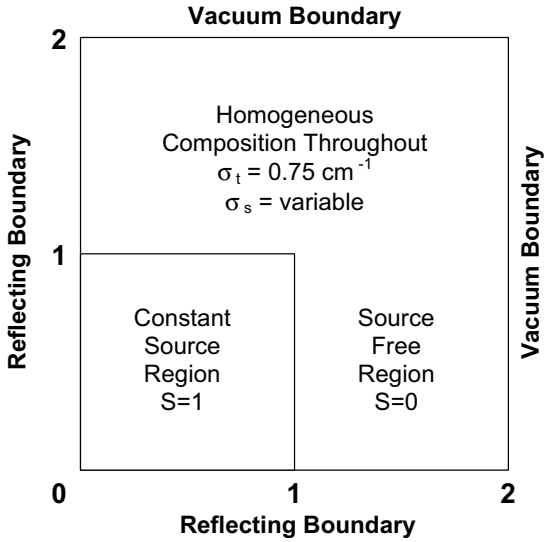

Figure 2. Benchmark ray effect problem.

MARCEL DEKKER, INC.
270 Madison Avenue, New York, New York 10016

where EPS is a user defined error measure (fixed to EPS $= 10^{-3}$ in the present study), Φ_i^n is the net particle density (scalar flux) evaluated at mesh cell i at iteration n and where ER is the error reduction achieved at iteration step n given by the ratio of the L-2 norms

$$\mathrm{ER} = \left\| \Phi^n - \Phi^{n-1} \right\|_2 / \left\| \Phi^{n-1} - \Phi^{n-2} \right\|_2, \quad \|u\|_2 = \left(\sum_i u_i^2 \right)^{1/2}. \quad (31)$$

The factor $1/(1-\mathrm{ER})$ is used in Eq. (30) to avoid false termination of the iterative solution process for slowly converging problems when the error reduction ER between successive steps is close to 1 (The error reduction ER is a positive number [by definition] which provides an estimate of the rate of convergence).

A small sample of the flux results is shown in Figures 3a–d, and in Table 7. Figures 3a–d show representative net flux contour plots and traverse plots at the last column ($x = 1.967$) of mesh cells. Table 7 shows error estimates of the flux solutions corresponding to various quadratures as compared with benchmark solutions. Table 7, Figures 3a–d, and other results omitted for brevity indicate the following:

(i) Figures 3a–b indicate that the standard S_{16} quadratures with 36 angles/octant lead to relatively large artificial flux fluctuations for the benchmark ray effect problem. Omitted results indicate that the fluctuations increase but their magnitudes decrease when the dg10111213 quadrature of Gelbard and Shure [6] with 46 angles/octant is used [1].

(ii) Figures 3c–d show that artificial flux fluctuations are substantially reduced with new quadratures such as s2468 with only 20 angles/octant. The fluctuations in Figures 3c–d are essentially eliminated with the new q461214 quadrature with 36 angles/octant.

The results in Figures 3a–d are qualitative and benchmarks are needed to assess accuracy. New quadratures dg4 × 20, sg4 × 20, d4 × 20, s4 × 20, q4 × 20 each having 4 cones and 20 angles/cone/octant for a total of 80 angles/octant, and s10 × 20, q10 × 20 each having 10 cones and 20 angles/cone/octant for a total of 200 angles/octant (see the definitions in Table 4), were developed and tested for their suitability as benchmarks. Single Gauss with 10 cones is essentially a P_{19} approximation along the polar z-direction, and this high order approximation is viewed to be a benchmark. In fact, the differences in answers start to get smaller and smaller for x–y problems as the number of cones around the z-axis is increased. The different quadratures having 10 cones and twenty angles per cone per octant produced essentially identical answers, as was expected. Omitted results indicate

MARCEL DEKKER, INC.
270 Madison Avenue, New York, New York 10016

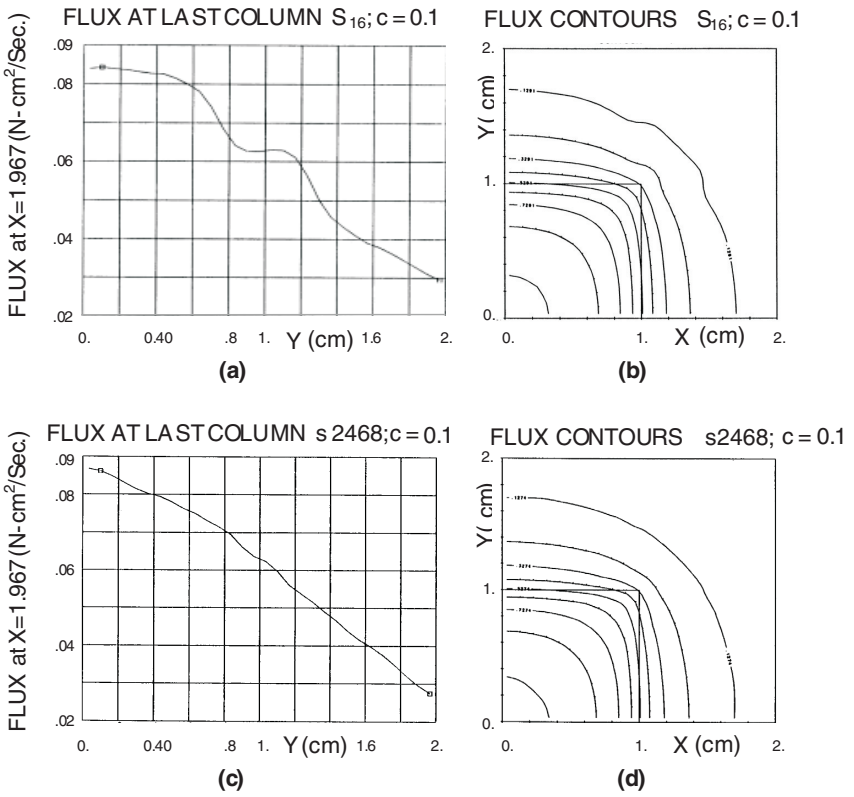

Figures 3. Edge flux and flux contours for problem 1 of Figure 2. (a)–(b). S_{16} Quadrature with 36 angles per octant, and (c)–(d). s2468 quadrature with 20 angles/octant and with 4 single-Gauss (SG) cones and respectively 2, 4, 6 and 8 new quadruple-range angles/octant quadratures distributed from top cone (closest to z-axis) to bottom cone (closest to x–y-plane).

the following:

(iii) The artificial flux fluctuations that are evident in the flux plots in most of Figures 3a–d are virtually non-existent when the s10 × 20 or q10 × 20 quadratures are used. Artificial flux fluctuations are also not evident when the q4 × 20, s4 × 20, or d4 × 20 quadratures are used (omitted results are much smoother than in Figures 3c–d). However, small artificial flux fluctuations still persist for the sg4 × 20 and dg4 × 20 where the 20 azimuthal angles are uniformly distributed on each of 4 single-Gauss and double-Gauss cones.

Table 7. Deviation of Edge Fluxes for the Ray Effect Problem of Figure 2 Corresponding to Various Quadratures from Edge Fluxes Corresponding to Benchmark Quadratures

Quadrature	Range of edge flux dzeviations	Quadrature	Range of ddge flux deviations
dg4444	−8% to 13%	dg2446	−8.0% to 11.2%
sg4444	−8% to 13%	sg2446	−7.1% to 9.6%
d4444	−11% to 10%	d2446	−5.8% to 4.3%
s4444	−11% to 10%	**s2446**[a]	**−5.2% to 5.5%**
		q2446	−5.3% to 5.7%
dg4466	−6.5% to 8.2%	dg2468	−6.5% to 7.5%
sg4466	−6.0% to 6.7%	sg2468	−5.1% to 5.6%
d4466	−5.9% to 5.0%	d2468	−7.2% to 3.5%
s4466	−6.5% to 3.7%	s2468	−4.8% to 2.3%
		q2468	**−4.3% to 2.1%**
dg881010	−3.3% to 3.3%	dg681012	−3.2% to 3.4%
sg881010	−3.5% to 2.9%	sg681012	−2.9% to 2.9%
d881010	−3.8% to 1.7%	d681012	−3.4% to 1.2%
s881010	−3.5% to 2.1%	s681012	−2.9% to 0.9%
		q681012	−2.7% to 1.0%
dg481014	−3.2% to 3.3%	dg461214	−3.6% to 3.5%
sg481014	−2.6% to 2.4%	sg461214	−2.8% to 2.5%
d481014	−2.6% to 1.3%	d461214	−3.1% to 1.4%
s481014	−1.1% to 1.1%	s461214	−1.4% to 1.0%
q481014	−0.8% to 1.6%	**q461214**	**−0.6% to 1.0%**
d241416	−4.8% to 3.0%	d241218	−5.0% to 2.9%
s241416	−2.2% to 1.3%	s241218	−2.2% to 1.3%
dg16	−7.5% to 8.0%	dg13121110	−2.3% to 2.3%
sg16	**−5.4% to 6.2%**	**sg13121110**	**−2.0% to 2.0%**
S_{16}	−7.0% to 7.7%	u13121110	−0.4% to 4.3%
q461820	−0.50% to 0.55%	**q681420**	**−0.37% to 0.53%**
q481620	**−0.56% to 0.32%**	q6101220	−1.2% to 0.44%
q4101420	−0.26% to 0.78%	q681618	−0.61% to 0.68%
		q6101418	−0.55% to 0.93%
dg4 × 20	−1.3% to 0.9%	d4 × 20	−0.34% to 0.01%
sg4 × 20	−1.3% to 0.8%	s4 × 20	−0.14% to −0.09%
		q4 × 20	**+0.01% to 0.05%**

[a]The best quadrature within each family is highlighted in bold face and is underlined.

This presents clear evidence that the QR distribution of azimuthal angles is vastly superior to the uniform Chebyshev–Gauss type distribution.

Omitted figures suggest that there is little difference between the results for the s10 × 20 and q10 × 20 quadratures, and between these 10 cone quadratures and the q4 × 20, s4 × 20 and d4 × 20 quadratures which have only 4 cones. To quantify the distinction between these and other quadratures, ratios of net fluxes were obtained and were plotted along the last row or column of the problem geometry. These last row or column locations are the furthest away from the source where differences typically have their maximum values. The ranges of deviation of edge fluxes corresponding to various quadratures from edge fluxes corresponding to benchmark s10 × 20 and q10 × 20 quadratures are listed in Table 7. The following observations and conclusions can be drawn based on Table 7, Figures 4a–b, and other results omitted for brevity:

(iv) Figure 4a shows ratios of boundary fluxes obtained with the q10 × 20, q4 × 20, s4 × 20 and d4 × 20 quadratures divided by boundary fluxes obtained with the s10 × 20 quadrature. This figure shows that the ratio of results for the q10 × 20 and s10 × 20 quadratures is essentially one everywhere. Furthermore, the ratio of the results for the q4 × 20 quadrature divided by those for the s10 × 20 quadrature varies between 1.0 and 1.0005 everywhere. These results confirm that either of the s10 × 20 and q10 × 20 quadratures, which produce virtually identical net fluxes, can be applied as a benchmark for our quadrature study. Furthermore, the use of 4 cones in the q4 × 20 quadrature leads to less than 0.05% difference from results obtained with the 10 cone benchmark quadratures. This is within solution convergence.

(v) Figure 4a further indicates that edge fluxes obtained with the s4 × 20 quadrature differ from benchmark results by about 0.14%. Likewise, edge fluxes obtained with the d4 × 20 quadrature differ from benchmark results by between 0.0% and 0.33%. In summary Figure 4a suggests that (a) the use of QR polar cone-based quadrature, as in the q4 × 20 quadrature, is to be preferred to the use of SG polar cone-based quadrature, as in the s4 × 20 quadrature. Further, this figure suggests that the use of the SG polar cone-based quadrature is to be preferred to the use of DG polar cone-based quadrature as in the d4 × 20 quadrature. This result is consistent with the comments on Figure 1b made in Section 5b above.

(vi) Figure 4b provides the ratios of the boundary fluxes obtained with the s4 × 20, d4 × 20, sg4 × 20, and dg4 × 20 quadratures divided by the corresponding results obtained with the benchmark s10 × 20 quadrature. The sg4 × 20 and dg4 × 20 quadratures result in fluctuations as was

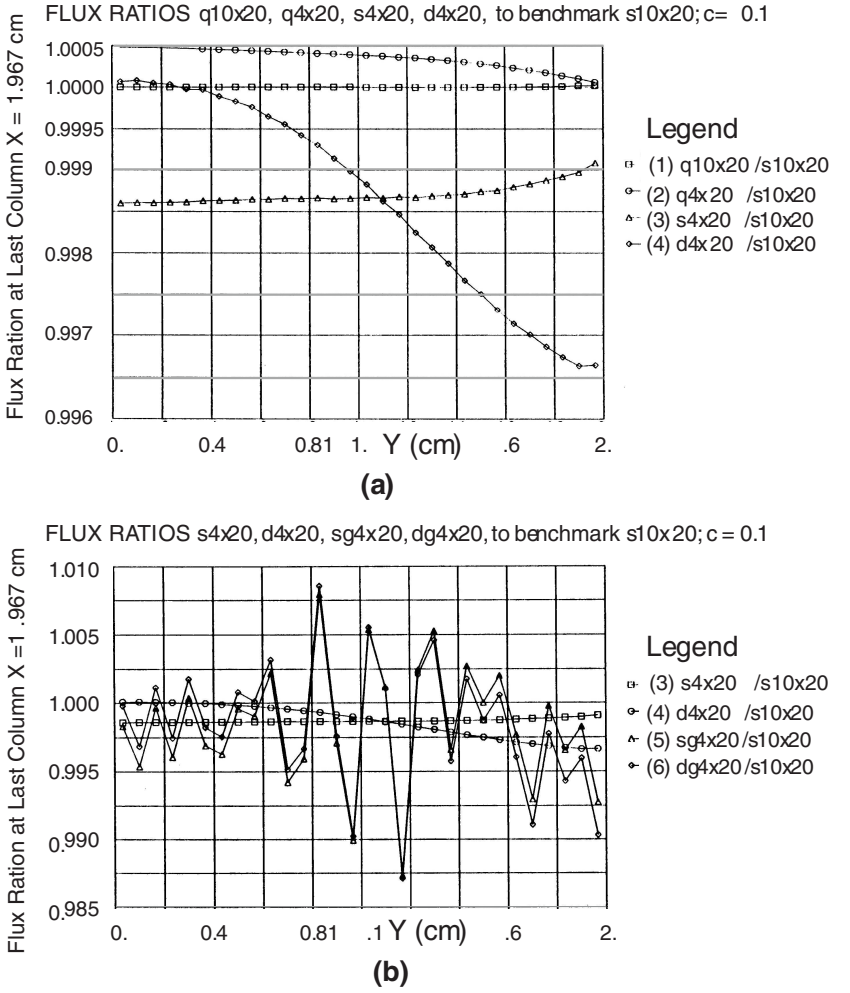

Figure 4. Ratios of edge fluxes at $X = 1.967$ evaluated as a function of different quadratures, divided by the edge fluxes corresponding to the benchmark s10 × 20 quadrature. (1) curve 1 q10 × 20 with 10 QR cones and 20 QR angles/cone/octant, (2) curve 2 q4 × 20 with 4 QR cones and 20 QR angles/cone/octant, (3) curve 3 s4 × 20 4 SG cones and 20 QR angles/cone/octant, (4) curve 4 d4 × 20 4 DG cones and 20 QR angles/cone/octant, (5) curve 3 sg4 × 20 4 SG cones and 20 uniform angles/cone/octant, and (6) curve 4 dg4 × 20 4 DG cones and 20 angles/cone/octant, each flux is divided by the benchmark flux corresponding to the s10 × 20 quadrature with 10 SG cones and 20 QR angles/cone/octant.

observed in item (iii) above. These fluctuations vary between -1.3% and 0.9% and Figure 4b again confirms that the use of QR azimuthal angles as in the s4 $\times$ 20 and d4 $\times$ 20 quadratures is superior to the use of uniformly distributed azimuthal angles as in the sg4 $\times$ 20 and dg4 $\times$ 20 quadratures.

Table 7 above, and other omitted results indicate the following:

(vii) Edge flux results corresponding to the standard S_{16} quadrature and the similar S_{16}-type, sg16 and dg16 quadratures have errors up to $\pm 8\%$.

(viii) The q461214 quadrature which has 4 QR cones is superior to the s461214 quadrature which has 4 SG cones, and the latter is superior to the d461214 quadrature which has 4 DG cones. Further, the sg461214 quadrature is definitely better than the dg461214 quadrature. Moreover, the latter two quadratures which have a uniform (Chebyshev–Gauss) distribution of azimuthal angles, are not competitive with the corresponding quadratures based on the QR distribution of azimuthal angles on each cone.

(ix) Among all the quadratures with 36 angles/octant considered in the present study, the q461214 quadrature yields the best results for the ray effect benchmark problem. The ordinates and weights for this quadrature are listed in Table 5. This quadrature should also be used for nuclear design and shielding applications to rectangular x–y transport problems, in place of the dg10111213 quadrature with 46 angles/octant recommended by Gelbard and Shure [6].

(x) Among the quadratures having 20 angles/octant, the q2468 quadrature is best. Furthermore, this quadrature is superior to the standard S_{16} quadrature which has 36 angles/octant. The ordinates and weights for this quadrature are listed in Table 6.

(xi) Among the qijkl quadratures having 46 angles/octant, the q481620 and q681420 quadratures yield the best results for the benchmark ray effect problem. These quadratures can be constructed from Tables 1, 3, and Algorithm 1, and are suitable for certain applications which require high order quadratures.

In summary, the QR quadratures for the azimuthal direction are superior to the standard Chebyshev–Gauss quadratures. Furthermore, for the polar direction, our numerical tests suggest that in most situations: (i) the choice of single-Gauss cones is better than double-Gauss cones, (ii) the choice of QR polar cones is comparable for low order quadrature to the choice of SG polar cones, and (iii) QR or OR polar cone-based quadratures yield better results than SG polar quadratures when high order formulas are applied. As was discussed above, the reason for the relatively poor behavior of the DG quadrature for x–y problems is most likely due to the fact that,

MARCEL DEKKER, INC.
270 Madison Avenue, New York, New York 10016

while double-Gauss has a bottom cone much closer to the x–y plane than the bottom SG or QR cones, the weight associated with the bottom DG cone is very small compared to that of the corresponding SG and QR cones. In other words, it is not only how close a cone is to the x–y plane that dominates and governs the transport in rectangular geometry, but what is more important is the combination of the relative position of a cone with respect to the x–y plane, and the weight associated with that position.

(b) Numerical results for benchmark x–y dry-cell storage problem

A model one-energy group P_3-scattering dry-cell storage x–y transport problem was set up by Dr. Kin Y. Cheung of Bettis, and was kindly provided by him to carry out a quadrature study. The problem configuration is shown in part in Figure 5a and is comprised of a localized uniform source placed in a very large air gap surrounded by a shield. The shield has a gap in it for access and a shield cover is placed at the end of the gap. The primary goal here is to accurately determine the neutron flux shape outside the gap. The flux of course can be used to determine dose rate and other parameters of interest to shield designers. For this quadrature study, the scale used for the view in Figures 5c,d is expanded along the y-direction for ease of distinguishing flux shapes in the region of interest corresponding to different angular quadrature formulas. This problem was extensively studied but results 1 1 are omitted for brevity. It is sufficient here to state the following:

(i) Exaggerated artificial flux fluctuations, not shown here for brevity, were obtained with the standard S_{16} angular quadrature, the Gelbard and Shure [6] angular quadrature, and several other quadratures including the dg4 $\times$ 20 quadrature with 80 angles/octant, as is evident from Figures 5b,c. These quadratures lead to large artificial flux fluctuations inside the access gap and in the region of interest outside the storage container, and that the fluctuations are more pronounced for directions nearly parallel to either the x-axis or y-axis.

(ii) Figures 5c,d clearly show that the choice of the d4 $\times$ 20 quadrature with quadruple-range distribution of azimuthal angles is considerably superior to the choice of dg4 $\times$ 20 quadrature with the same number of angles/octant but with uniform Chebyshev–Gauss distribution of azimuthal angles. However, flux fluctuations still persist, which suggests the need for higher order or specialized quadratures for this dry-cell storage problem [1]. Further details are beyond the scope of this paper.

MARCEL DEKKER, INC.
270 Madison Avenue, New York, New York 10016

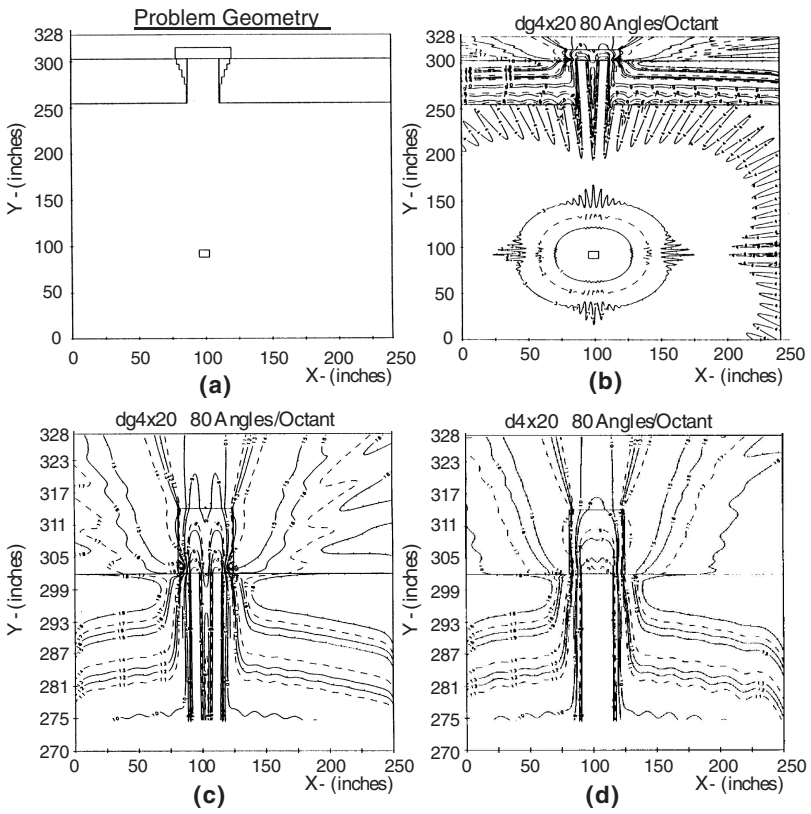

Figures 5. Geometry and group 1 flux contours for model dry-cell storage problem. (a) Complete problem geometry, (b)–(c) Flux contours and Y-expanded section of their top part for the dg4 × 20 quadrature [4 DG cones, 20 uniformly distributed angles/cone/octant], and (d) Expanded top part of flux contours for the d4 × 20 quadrature [4 DG cones but with 20 quadruple-range azimuthal angles/cone/octant].

7. SUMMARY

Low order angular quadrature formulas which allow for possible discontinuities at material interfaces in 2-D rectangular x–y geometries were previously developed and demonstrated to be effective in ameliorating artificial ray effect flux fluctuations, and in improving accuracy [2]. The present paper extends the quadruple-range quadratures developed for azimuthal integration from order N=7 in previous published work [2] to N=22.

MARCEL DEKKER, INC.
270 Madison Avenue, New York, New York 10016

This paper also generalizes the development in Ref. [2] to apply to 3-D rectangular problems. Separate quadrature formulas are developed and tabulated for the polar and azimuthal integrations of the scattering term of the particle transport equation. Octant-range quadratures can be constructed by selecting a single quadrature for the polar integration, and allowing possibly different quadrature formulas for the azimuthal integration along each of the separate discrete levels (cones) of the polar quadrature. As a consequence, improved accuracy was achieved with far fewer quadrature points as compared to previous work [2], resulting in considerable computational economy. New angular quadratures suitable for general x–y problems that arise in nuclear and shield design and analysis are identified.

ACKNOWLEDGMENTS

The ideas for the present work evolved during the past twenty-five years as the author was responding to requests for improved accuracy of discrete ordinates transport theory computational methods. Several individuals contributed to the effort of testing the quadratures for their applications, providing feedback, and where appropriate, writing or co-authoring local reports. Much of the credit and thanks are due to current and former colleagues, including Norm Candelore, Kin Cheung, Lou Hageman, Melissa Hunter, Roger Martz, Tom Pitcairn, Joel Risner, Ron Selva, Kal Shure, Joe Wallace, Joni Winwood, Carl Yehnert and Mike Zerkle. The author is also grateful for the help received from Jim Dankosky and Larry Foulke who have motivated and continue to motivate the search for improved transport methods and who have made writing this paper possible. This work was supported by the U.S. Department of Energy under contract DE-AC11-98PN38206.

REFERENCES

1. I. K. Abu-Shumays, "Angular Quadratures for Improved Transport Computations," Bettis Atomic Power Laboratory Report B-T-3276, West Mifflin, Pennsylvania, July 22, 1999. Available from the US DOE Office of Scientific and Technical Information (OSTI), Oak Ridge, Tennessee.
2. I. K. Abu-Shumays, "Compatible Product Angular Quadrature for Neutron Transport in x–y Geometry," *Nucl. Sci. Eng.*, **64**, 299–316, 1977.

3. I. K. Abu-Shumays, ''Low-Order Gauss–Christoffel Quadrature,'' Argonne National Laboratory Report ANL-7914, February 1972.
4. B. G. Carlson, ''Tables of Equal Weight Quadrature EQ_n over the Unit Sphere,'' Los Alamos Scientific Laboratory Report LA-4734, July 1971.
5. W. Gautschi, ''Construction of Gauss–Christoffel Quadrature Formulas''. *Math. Comput.*, **22**, No. 102, pp. 251–270, April 1968.
6. E. M. Gelbard, ''Arrangement of Ordinates in Deep Penetration Cylindrical and x–y S_n Calculations,'' In Proc. Conf. ''New Developments in Reactor Mathematics and Applications'', CONF-710302 (Vol. 2), Idaho Falls, Idaho, March 29–31, 1971.
7. K. D. Lathrop, ''Elimination of Ray Effects by Converting Discrete Ordinate Equations to Spherical Harmonic-Like Equations,'' In Proc. Conf. ''New Developments in Reactor Mathematics and Applications,'' CONF-710302 (Vol. 2), Idaho Falls, Idaho, March 29–31, 1971.
8. K. D. Lathrop and B. G. Carlson, ''Discrete Ordinates Angular Quadrature of the Neutron Transport Equation,'' Los Alamos Scientific Laboratory Report LA-3186, February 1965.
9. A. H. Stroud and D. Secrest, *Gaussian Quadrature Formulas*, Prentice-Hall, Inc., Englewood Cliffs, N.J., (1966).

Received July 26, 1999
Revised August 1, 2000
Accepted October 2, 2000